Supplementary Information for

Tip-induced bond weakening, tilting, and hopping of a single CO molecule on Cu(100)

Xiao-Ru Dong[1,†], Ben Yang[1,†], Rui Zhu[1], Rui-Pu Wang[1], Yang Zhang[1], Yao Zhang[1,*] and Zhen-Chao Dong[1,*]

[1]Hefei National Research Center for Physical Sciences at the Microscale and Synergetic Innovation Centre of Quantum Information & Quantum Physics, University of Science and Technology of China, Hefei, Anhui 230026, China

[*]Corresponding authors. Email: zhy2008@ustc.edu.cn; zcdong@ustc.edu.cn

[†]Equally contributed to this work.

Content

S1 TERS measurements in the low-frequency region

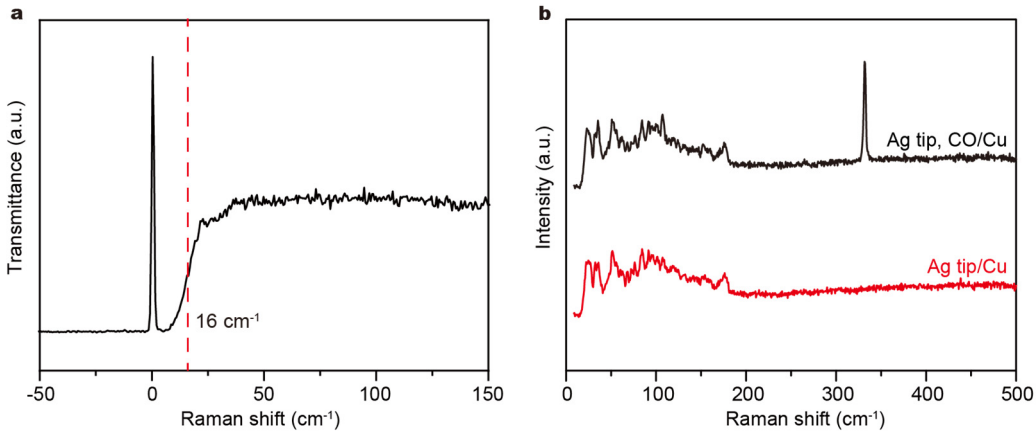

Fig. S1 TERS measurements in the low-frequency region. a, Optical transmittance of the TERS setup by illuminating the junction with both the 532 nm laser and the write light simultaneously. **b,** TERS spectra acquired at CO/Cu(100) and bare Cu(100) surface in the low-frequency region.

The detection limit for TERS measurements in the low-frequency region mainly depends on both the optical resolution of the spectrometer used and the steepness of cut-off edge for the Nano-edge filters. In our measurements, the spectrometer with a focal length of 320 mm (IsoPlane SCT320, Princeton Instruments), a slit size of 50 μm and a grating of 2400 grooves per mm were used to achieve an optical resolution of ~2.2 cm^{-1}. The experimental setup for low-frequency TERS measurements is shown in Fig.1 in the main text, in which the use of the Nano-edge and BPF filters with steep cut-off edges are the key to measure the low-frequency Raman vibrational signals[1]. As shown in Fig. S1a, the optical transmittance through two Nano-edge filters by simultaneously illuminating both the 532 nm laser and the white light into the junction is collected to characterize the detection limit of our TERS setup in the low-frequency region less than 500 cm^{-1}. The lowest frequency we can detect is about 16 cm^{-1} relative to the laser excitation energy estimated by the energy position at half of the whole intensity jump (red dashed line in Fig. S1a), which is sufficient to measure the frustrated rotation (FR) mode of CO on Cu(100) at ~288 cm^{-1} and the frustrated translational (FT) mode at ~32 cm^{-1} deduced from IETS results[2]. Figure S1b shows the TERS spectra acquired at CO/Cu(100) for frequency ranges less than 500 cm^{-1}. The Raman peak centered at 332 cm^{-1} is assigned to the Cu–CO stretching vibration and the Raman peaks at less than 200 cm^{-1} can be attributed to the vibrations of atomic-scale Ag clusters at the apex of the Ag tip[3] since these Raman peaks are nearly identical in terms of the peak positions and intensities for the TERS measurements on both the CO molecule and bare Cu(100) surface. In other words, both the FT mode and the FR mode, are completely absent in the TERS spectrum of CO on Cu(100), which is consistent with the TERS selection rule since these two vibrational modes are assigned to the in-plane modes along the surface plane.

S2 Estimation on the gap distances at different currents and biases

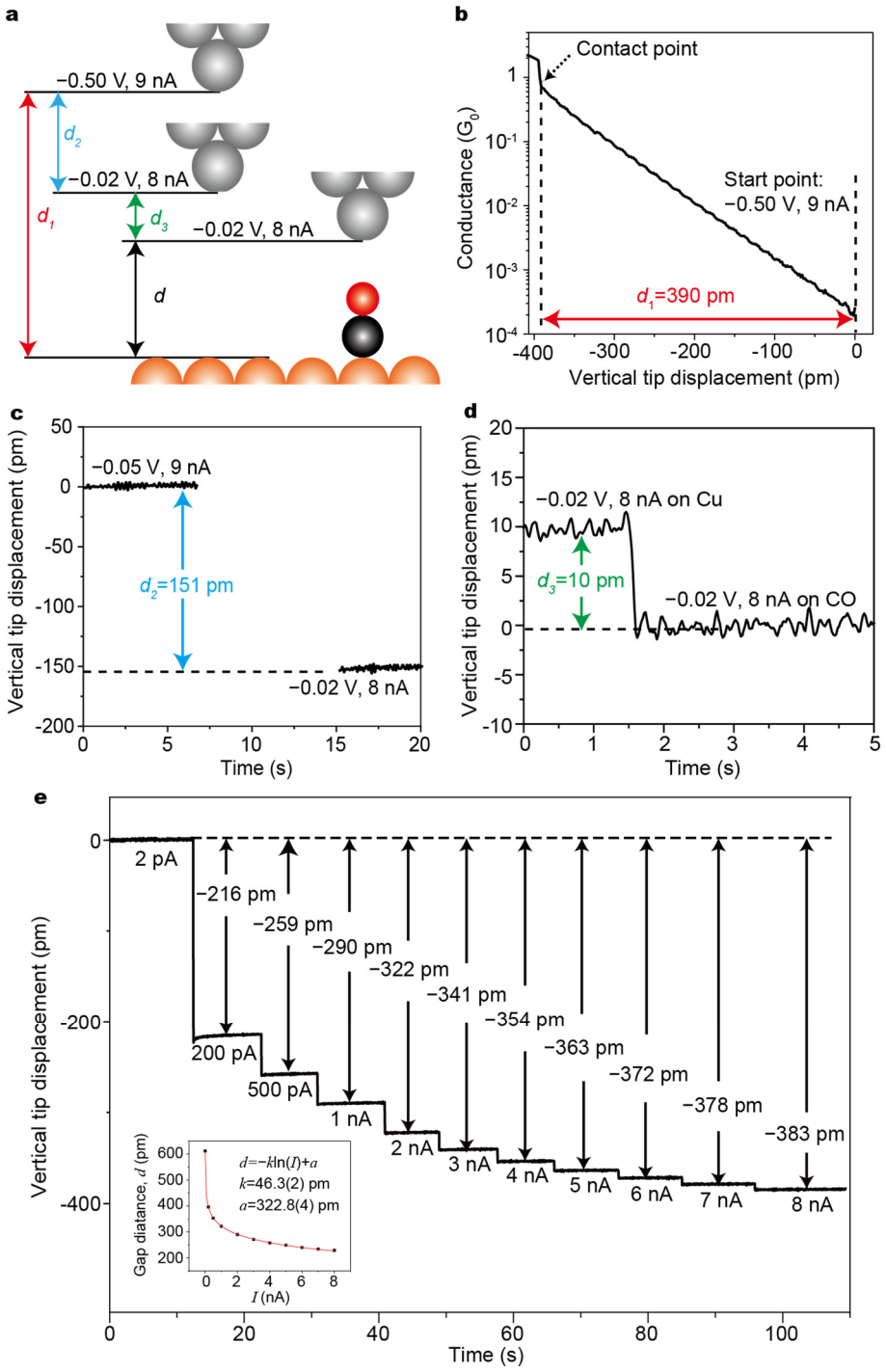

Fig. S2 Measurements of gap distances at different currents for a given bias of −0.02 V. a, Schematic illustrating various gap distances in the STM junction. **b**, Tip trajectory during the approaching to the Cu substrate from an initial setpoint (−0.50 V, 9 nA) to the contact point. **c**, Distance variations when switching the scanning condition from −0.50 V, 9 nA to −0.02 V, 8 nA. **d**, Apparent height of a single CO molecule adsorbed on Cu(100) under the tunneling condition of −0.02 V and 8 nA. **e**, Variations in the gap distances at a given bias of −0.02 V but with different currents from 2 pA to 8 nA.

As illustrated in Fig. S2a, the gap distance d for the tunneling condition of −0.02 V and 8 nA, as a reference for obtaining the gap distances at different currents, is estimated through the measurements of the tip trajectories with different tunneling conditions[4], and can be expressed as $d=d_1-d_2-d_3$, with d_1, d_2, and d_3 distances defined in the figure. Here the zero point of the gap distance (d) is defined as the position when the tip apex atom contacts to the substrate atoms with the conductance reaching the conductance quantum G_0. As shown in Fig. S2b, the gap−distance d_1 for the tunneling condition of −0.5 V and 9 nA is measured through a controlled tip−substrate contact using a low-gain pre-amplifier setting (10^5 V·A^{-1}). The distance difference (d_2) between the tip positions for two different scanning conditions of (−0.50 V, 9 nA) and (−0.02 V, 8 nA) is measured using a high-gain pre-amplifier setting (10^9 V·A^{-1}) and the height variation in Fig. S2c shows that d_2 is about 151 pm. The apparent height d_3 of a single CO molecule for the tunneling condition of −0.02 V, 8 nA is about 10 pm in Fig. S2d. Therefore, we can estimate the gap−distance for the tunneling condition of −0.02 V and 8 nA to be about 229 pm (i.e., d=390−151−10=229 pm). By using the measured height variations between different currents (2 pA to 8 nA) with a bias at −0.02 V, as shown in Fig. S2e, we can further estimate the gap distance at those different currents. Moreover, for the tunneling currents which are not included in Fig. S2e, the corresponding gap distance can also be obtained through the nice exponential fit shown in the inset via $d=-k\ln(I)+a$, with a decay constant of k=46.3(2) pm.

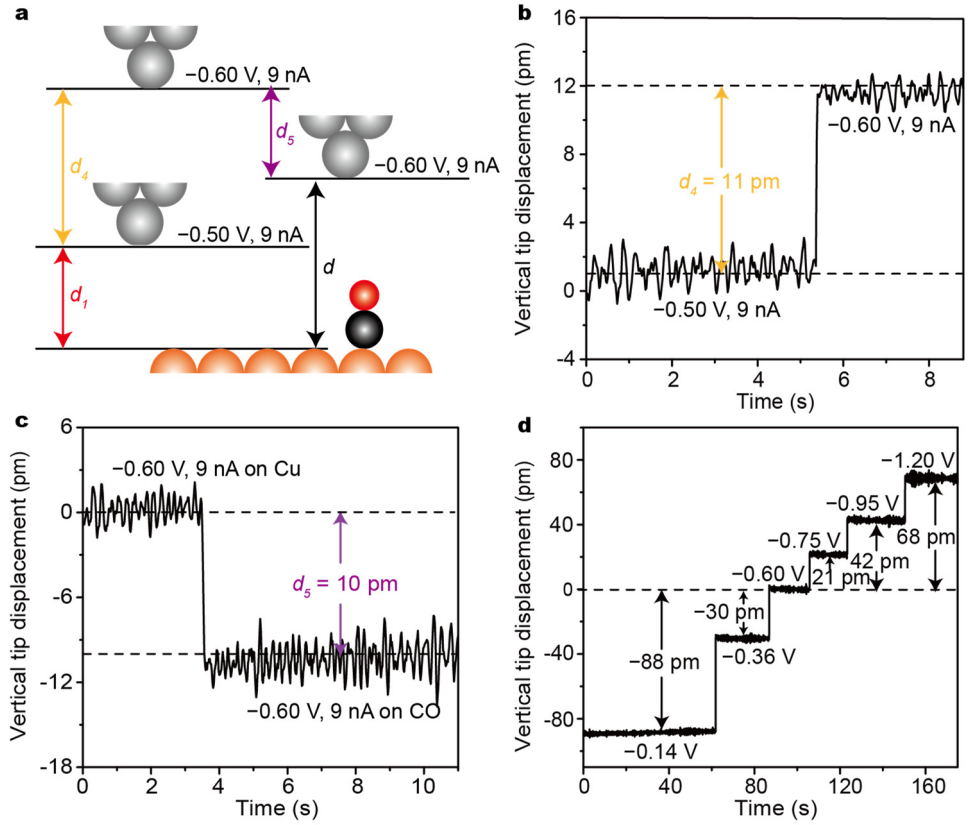

Fig. S3 Measurements of gap distances at different biases for a given current of 9 nA. a, Schematic illustrating various distances in the STM junction. **b,** Distance variations from the scanning condition of −0.50 V, 9 nA to −0.60 V, 9 nA. **c,** Apparent height of a single CO molecule adsorbed on Cu(100) under −0.60 V and 9 nA. **d,** Variations in the gap distances for different biases ranging from −0.14 V to −1.20 V at a fixed current of 9 nA.

In order to obtain high signal-to-noise ratio spectra for different gap distances in main-text Fig. 3b, different biases with a large but fixed current of 9 nA are used to control the gap distance. As illustrated in Fig. S3a, the gap distance d at the condition of −0.6 V and 9 nA, used as a reference position, is estimated through the measurements of the tip trajectories with different conditions, and can be expressed as $d=d_1+d_4-d_5$. As shown in Fig. S3b, the distance difference (d_4) between the tip positions from −0.50 V and 9 nA to −0.60 V and 9 nA is about 11 pm. The apparent height (d_3) of a single CO molecule adsorbed on the Cu(100) substrate for the tunneling condition of −0.60 V and 9 nA is about 10 pm in Fig. S3c. Therefore, we can deduce the gap distance for the tunneling condition of −0.6 V, 9 nA to be about 391 pm (*i.e.*, $d=d_1+d_4-d_5$=390+11−10=391 pm). Then, by comparing the measured height variations between different bias conditions from −0.14 V to −1.20 V with a fixed current of 9 nA, as shown in Fig. S3d, we can estimate the gap distances at those biases.

S3 Calculated bond lengths and Raman frequencies of a CO molecule adsorbed on Cu(100) with different gap distances

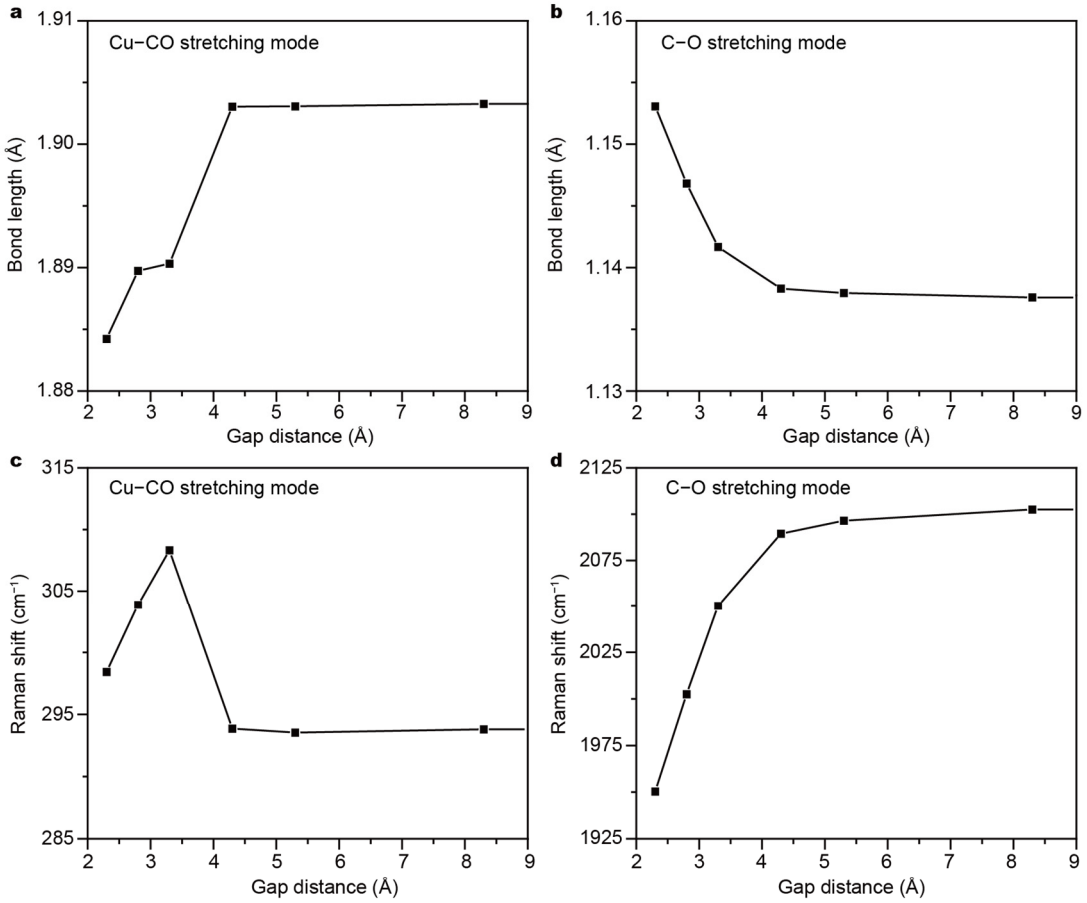

Fig. S4 Calculated bond lengths and stretching frequencies for Cu−CO and C−O bonds at different gap distances. a, Cu−CO bond lengths. **b,** C−O bond lengths. **c,** Cu−CO stretching frequencies. **d,** C−O stretching frequencies.

The comparison of the calculated Cu−C and C−O bond lengths as well as the corresponding stretching vibration frequencies with varying gap distances is shown in Fig.S4. As the tip approaches from far away to 2.3 Å to the substrate, the changes of Cu−CO bond length from 1.903 Å to 1.884 Å (relatively changed by 0.99 %) is a little smaller than the changes of the C−O bond length from 1.138 Å to 1.153 Å (relatively changed by 1.36%). The simulated vibrational frequency for Cu−CO stretching mode only red shifted by ~4 cm^{-1} as the tip approaches, which is much smaller than the shift of C−O stretching mode (~152 cm^{-1}) and qualitatively consistent with the experimental results. Note that the frequency shift for the Cu−CO stretching mode does not have a simple monotonous relation to the bond length as the tip is getting very close to the molecule. The CO tilting angle also plays a role here. All the structural optimizations, vibrational calculations and electronic properties are simulated by the hybrid B3LYP functional with Grimme's DFT-D3 correction[5] and the 6-311++G(d, p) basis set for C

and O atoms and lanl2dz basis set for Cu and Ag atoms in the Gaussian16 software[6]. The tip contains 10 Ag atoms and the substrate contains 42 Cu atoms. All the structures are of closed shell, and only the CO molecule and the bonded Cu atom is optimized while the other metal atoms are kept frozen. The electronic density difference in main-text Fig. 3f is obtained from $\Delta\rho = \rho_{tip+CO+Cu} - \rho_{tip} - \rho_{CO} - \rho_{Cu}$, where $\rho_{tip+CO+Cu}$ is the total electronic density of the whole system and $\rho_{tip/CO/Cu}$ is the electronic density of the isolated tip/CO/Cu, respectively.

S4 Optimized structures of a CO molecule adsorbed on Cu(100) with different gap distances

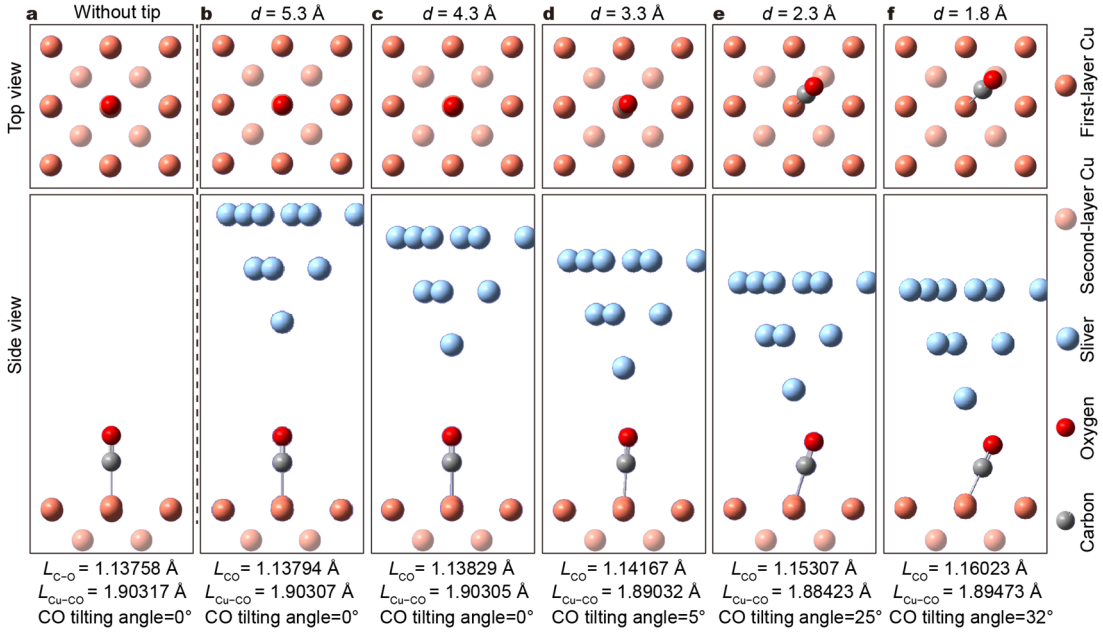

Fig. S5 Optimized structures of an adsorbed CO molecule on Cu(100) with different gap distances. a, Top view (**top panel**) and side view (**bottom panel**) showing a CO molecule vertically adsorbed on the Cu (100) surface without a tip. **b-f**, Top view (**top panel**) and side view (**bottom panel**) of a CO molecule adsorbed on Cu(100) at different gap distances. The adsorbed CO molecule starts to tilt along the [110] direction when the gap distance is smaller than ~3.9 Å, which corresponds to an inter-atomic distance of ~3.6 Å between the Ag atom at the tip apex and the O atom of the CO molecule and is very close to the Ag···O van der Waals distance of ~3.65 Å[7]. Here the zero point of the gap distance (*d*) is again defined as the position when the tip apex atom contacts to the substrate atom, similar to the definition used in Fig. S2. The radius for the Cu atom at the substrate and the Ag atom at the tip apex, with a sum of $r_{Cu} + r_{Ag}$ ~2.7 Å, is not take into account in the estimation of the gap distance. The variations in the C−O bond lengths, Cu−CO bond lengths and the CO tilting angles are listed under each configuration. Note that the separation between the surface Cu atom and the O atom of the CO molecule is about 3 Å according to the simulations, which is used in the estimation of CO tilting angles.

S5 Natural bond orbital (NBO) analysis of a CO molecule adsorbed on the Cu(100) surface

Table S1. NBO analysis of an adsorbed CO molecule on Cu(100) with different gap distances

Gap distances	Donor	Type	*ED* (*e*)[a]	Acceptor	Type	*ED* (*e*) [a]	*E*(2) (kJ·mol^{-1}) [b]
8.3 Å	Cu	d_{xz}	1.94610	C	p_x	0.60375	8.81
	Cu	d_{yz}	1.94610	C	p_y	0.60375	8.81
5.3 Å	Cu	d_{xz}	1.94592	C	p_x	0.60370	8.87
	Cu	d_{yz}	1.94592	C	p_y	0.60370	8.87
4.3 Å	Cu	d_{xz}	1.94572	C	p_x	0.60337	8.88
	Cu	d_{yz}	1.94572	C	p_y	0.60337	8.88
	Ag	*s*	0.84884	CO	σ^*	0.01299	0.12
3.3 Å	Cu	d_{xz}	1.94347	C	p_x	0.60414	6.78
	Cu	d_{yz}	1.94337	C	p_y	0.60513	6.77
	Cu	d_{xz}	1.94347	C	p_y	0.60513	2.60
	Cu	d_{yz}	1.94337	C	p_x	0.60414	2.60
	$Cu_{Near,1}$	d_{z^2}	1.98747	C	p_y	0.60513	0.11
	$Cu_{Near,1}$	d_{yz}	1.97949	C	p_y	0.60513	0.11
	$Cu_{Near,2}$	d_{z^2}	1.98712	C	p_x	0.60414	0.17
	$Cu_{Near,2}$	d_{xz}	1.97956	C	p_x	0.60414	0.20
	$Cu_{Near,3}$	d_{z^2}	1.98732	C	P_y	0.60513	0.15
	$Cu_{Near,3}$	d_{yz}	1.97957	C	p_y	0.60513	0.15
	$Cu_{Near,4}$	d_{z^2}	1.98761	C	p_x	0.60414	0.10
	$Cu_{Near,4}$	d_{xz}	1.97943	C	p_x	0.60414	0.08
	Ag	*s*	0.77792	CO	σ^*	0.01562	2.19
2.3 Å	Cu	d_{xz}	1.94202	C	p_x	0.65600	7.73
	Cu	d_{yz}	1.93807	C	p_y	0.64576	9.76
	Cu	d_{z^2}	1.95021	C	p_x	0.65600	2.21
	$Cu_{Near,1}$	d_{xz}	1.97294	C	p_x	0.65600	0.52
	$Cu_{Near,1}$	d_{yz}	1.97768	C	p_y	0.64576	0.63
	$Cu_{Near,2}$	d_{xz}	1.97294	C	p_x	0.65600	0.53
	$Cu_{Near,2}$	d_{yz}	1.97767	C	p_y	0.64576	0.62
	Ag	*s*	0.70095	CO	σ^*	0.01915	4.75

[a]*ED* is the electron density (i.e., occupancy) of corresponding orbital.

[b]*E*(2) is the stabilization energy of hyper-conjugative interaction between donor and acceptor.

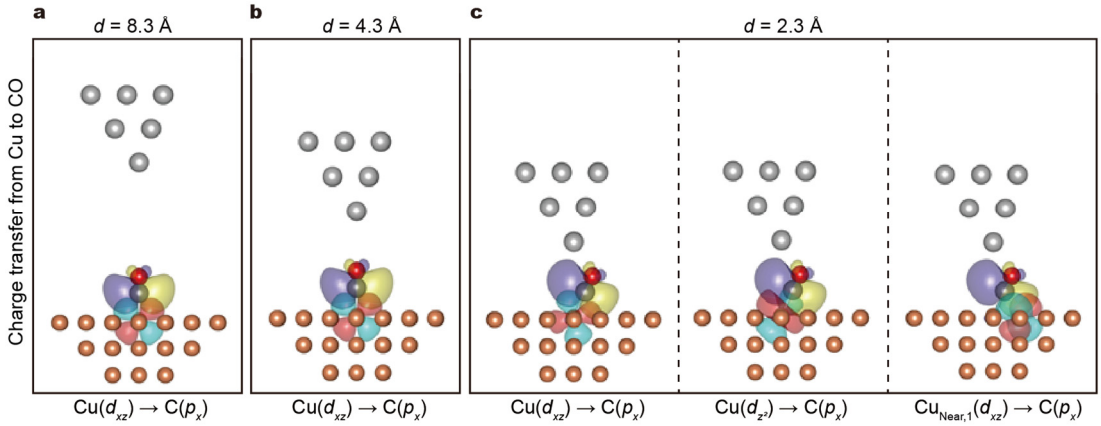

Fig. S6 Donor and acceptor orbitals at representative gap distances to show the increasing interactions (overlaps) between the CO molecule and Cu substrate as the tip approaches.

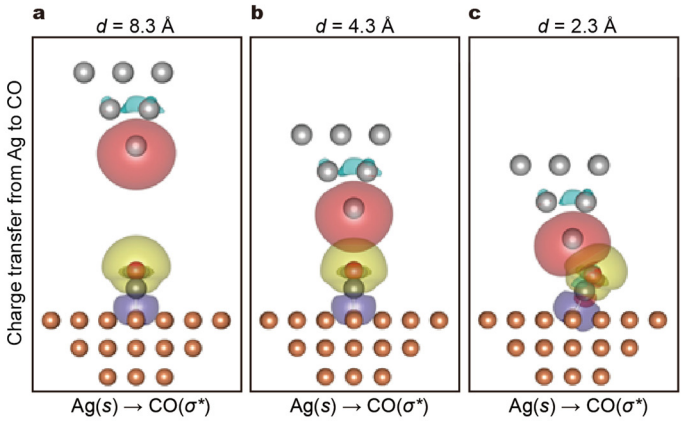

Fig. S7 Donor and acceptor orbitals at representative gap distances to show the increasing interactions (overlaps) between the CO molecule and Ag tip as the tip approaches.

We have performed additional simulations for NBO analysis using the same simulation functional and basis set in Section S3. Table S1 shows the summarized results from the NBO analysis of an adsorbed CO molecule on the Cu(100) surface with different gap distances. As long as the Ag tip is far enough (> 5 Å), the electrons are mainly transferred from the d_{xz} and d_{yz} orbitals of the Cu atom to the p_x and p_y orbitals of C atom bonded with it. As the gap distance decreases, both the d_{z^2} orbital of the bonded Cu atom and the *d* orbitals of the neighboring Cu atoms will be involved in the charge transfer process (Fig. S6), resulting in more occupations (increasing in electron densities) in the *p* orbitals of the C atom in the CO molecule. Moreover, the contribution from the *s* orbital of the apex Ag atom to the σ^* orbital of CO also increases as the tip approaches (Fig. S7). All these results support our claim that such a tilting would result in more charge transfer from the substrate to the antibonding $2\pi^*$ orbitals of the CO molecule.

S6 Theoretical simulations by moving the Ag tip over the CO molecule along the [110] direction of the Cu(100) surface

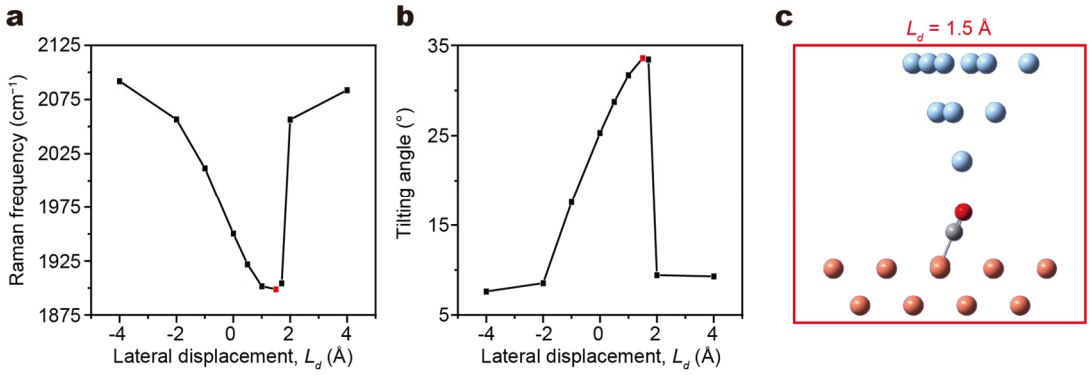

Fig. S8 The C−O stretching frequency, tilting angle and tip position during the scanning process. a, b, Dependence of C−O stretching frequency (**a**) and tilting angle (**b**) of an adsorbed CO molecule with the lateral displacement of the Ag tip along the [110] direction of the Cu(100) surface. **c,** Molecular geometry corresponding to the minimum frequency labelled in **a** and **b**, where the tip apex is right above the oxygen atom of the adsorbed CO molecule.

In order to provide a better justification to determine the correspondence between the minimum frequency and the C or O position, we have performed additional theoretical simulations by moving the Ag tip over the CO molecule along the [110] direction of the Cu(100) surface at a fixed gap distance of 2.3 Å. The variations of tilting angles and C−O stretching vibrational frequencies are plotted in Fig. S8, and the geometry of the molecular system around the minimum frequency are also shown. Apparently, the Ag tip apex is right above the oxygen atom when the C−O stretching frequency attains the minimum and the CO tilting angle reaches the maximum. Therefore, it is reasonable to regard the minimum frequency position in the TERS map of Fig. 4f to correspond to the position of the oxygen atom and estimate the tilting angles of the CO molecule.

S7 Tip-induced hopping of the CO molecule along the [100] or [010] direction of the Cu(100) surface

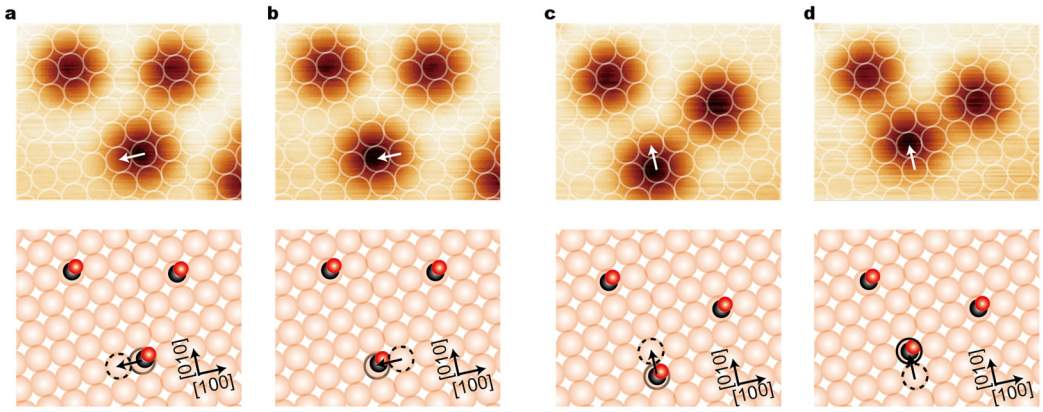

Fig. S9 Tip-induced hopping of the CO molecule along the [100] or [010] direction of the Cu(100) surface. a, b, Before-manipulation (**a**) and after-manipulation (**b**) STM image (top) and schematic of the corresponding adsorption position (bottom) for single CO molecules on one area of the Cu(100) surface. The bottom single CO molecule on Cu(100) hops to the nearest Cu atom via the bridge site along the [−100] direction. **c, d,** Before-manipulation (**c**) and after-manipulation (**d**) STM image (top) and schematic of the corresponding adsorption position (bottom) for single CO molecules on another area of the Cu(100) surface. The bottom single CO molecule on Cu(100) hops to the nearest Cu atom via the bridge site along the [010] direction. The molecular manipulation shown here was performed by first positioning the tip above the CO molecule at a setpoint of –0.1 V and 200 pA, then switching off the feedback loop and approaching to the molecule by 360 pm, and finally laterally moving the tip to the boundary of the molecule. The gap distance at the moment of molecular pushing here is estimated to be about 102 pm, enough to induce the first jump shown in main-text Fig. 5c. The observed manipulation results give further support to the hopping pathway of a CO molecule via the bridge site to the nearest Cu neighbor along the [100] or [010] direction. However, we do not observe the status of CO molecules being adsorbed on the bridge site, which can be understood from previous reports that the bridge site is just a metastable state with a very shallow minimum (< 25 meV)[8].

References

1 Lin, M. L. *et al.* Ultralow-frequency Raman system down to 10 cm^{-1} with longpass edge filters and its application to the interface coupling in t(2+2) LGs. *Review of Scientific Instruments* **87**, 053122 (2016).

2 Lauhon, L. J. & Ho, W. Single-molecule vibrational spectroscopy and microscopy: CO on Cu (001) and Cu (110). *Physical Review B* **60**, R8525-R8528 (1999).

3 Zhang, X. B. *et al.* Fast fabrication and judgement of TERS-active tips. *Chinese Journal of Chemical Physics* **35**, 713-719 (2022).

4 Yang, B. *et al.* Sub-nanometre resolution in single-molecule photoluminescence imaging. *Nature Photonics* **14**, 693-699 (2020).

5 Grimme, S. *et al.* A consistent and accurate ab initio parametrization of density functional dispersion correction (DFT-D) for the 94 elements H-Pu. *The Journal of Chemical Physics* **132**, 154104 (2010).

6 Frisch, M. *et al.* Gaussian 16, Revision A. 03; Gaussian: Wallingford, CT, USA, 2016.

7 Batsanov, S. S. Van der Waals radii of elements. *Inorganic Materials* **37**, 871-885 (2001).

8 Wei, Z. Y., Göltl, F. & Sautet, P. Diffusion barriers for carbon monoxide on the Cu (001) surface using many-body perturbation theory and various density functionals. *Journal of Chemical Theory and Computation* **17**, 7862-7872 (2021).